PROCEEDINGS OF SCIENCE

ONLINE ICRC 2021
THE ASTROPARTICLE PHYSICS CONFERENCE
Berlin | Germany
37th International Cosmic Ray Conference
12–23 July 2021

Very-forward π^0 production cross section in proton-proton collisions at $\sqrt{s}$ = 13 TeV measured with the LHCf experiment

Alessio Tiberio[a,*] **on behalf of the LHCf Collaboration**
(a complete list of authors can be found at the end of the proceedings)

[a] *INFN, section of Florence*
Via Bruno Rossi 1, Sesto Fiorentino (FI), Italy
E-mail: alessio.tiberio@fi.infn.it

The LHCf experiment, situated at the LHC accelerator, is composed of two independent detectors located at 140 metres from the ATLAS interaction point (IP1) on opposite sides along the beam axis. LHCf covers the pseudorapidity region above 8.4, with the capability to measure zero-degree neutral particles. The physics motivation of the experiment is to test the hadronic interaction models commonly used in ground-based cosmic rays experiments to simulate air-showers induced by ultra-high-energy cosmic rays (UHECR) in the Earth atmosphere. The data from accelerator experiments are very important for the tuning of these phenomenological models in order to reduce the systematic uncertainty of UHECR measurements. A precise measurement of the π^0s produced in the very-forward region in high energy collisions provides the possibility to study the electromagnetic component of secondary particles produced in the first interaction of a UHECR with the atmosphere. In this contribution the preliminary results from the π^0 analysis of the data acquired in proton-proton collisions at $\sqrt{s}$ = 13 TeV will be presented. The Feynman-x and transverse momentum spectra obtained with the two detectors will be compared to show the consistency of the results.

37th International Cosmic Ray Conference (ICRC 2021)
July 12th – 23rd, 2021
Online – Berlin, Germany

*Presenter

PoS(ICRC2021)386

1. Introduction

The observation of Ultra-High-Energy Cosmic Rays (UHECR) is carried out by ground-based experiments with large arrays of detectors, as the Pierre Auger Observatory [1] and the Telescope Array [2]. The detection technique of the UHECRs is based on the observation of the shower of secondary particles produced in the interaction of the cosmic rays with a nucleus of the atmosphere (the so-called "air-showers"). Accurate Monte Carlo simulations are therefore required to extract the astrophysical parameters of the primary cosmic ray from the air-shower observables. Ground based experiments have already published results of observables sensitive to the chemical composition of the UHECRs [3, 4], but a clear interpretation of the data is made difficult because of the large systematic uncertainty associated to the disagreement between different hadronic interaction models employed in the simulations. Since hadronic interaction models commonly used in air-shower simulations are phenomenological models based on the Gribov-Regge theory [5, 6], the tuning of these models with experimental data is fundamental to reduce the systematic uncertainty of UHECR measurements. The Large Hadron Collider (LHC [7]) provides the highest energy available at an accelerator and grants an unique opportunity for the tuning of hadronic interaction models and reduce the uncertainty of their extrapolation at UHECR energies (> 10^{18} eV). The LHC-forward (LHCf [8]) experiment is designed to measure the very-forward neutral particles production at the LHC, in particular photons, neutrons and π^0s. The very-forward region covered by LHCf (at pseudorapidity $\gtrsim$ 8.4) is crucial for the tuning of air-shower hadronic interaction models, since it is the region where most of the energy flow of the secondary particles is concentrated. LHCf has carried out measurements in proton-proton collisions at $\sqrt{s}$ = 0.9, 2.76, 7 and 13 TeV, and in proton-lead collisions at $\sqrt{s_{NN}}$ = 5.02 and 8.16 TeV [9–17].

A description of the experimental apparatus of LHCf is given in Section 2. The reconstruction procedure of a π^0 event is explained in Section 3. The preliminary results of the analysis, showing the transverse momentum distribution in several Feynman-X bins are discussed in Section 4.

2. The LHCf experiment

The LHCf experiment is composed of two independent detectors (named "Arm1" and "Arm2") placed ~140 meters away from the Interaction Point 1, on opposite sides. The detectors are placed in the Target Absorber Neutral (TAN) instrumentation slot, where the unique beam pipe from the interaction point is splitted into the two beam pipes of the colliding beams. The position between the two beam pipes permits to measure particles emitted at a pseudorapidity $\gtrsim$ 8.4, up to zero-degree particles. Since charged particles are deflected by the dipole magnets which bend the colliding beams into their own beam pipes, only neutral particles can be measured by the detectors. Each detector is made of two sampling and position sensitive calorimeters (called "towers" hereafter). GSO scintillators are used as active layers, while tungsten is used as absorber. All the calorimeters have a depth of 44 radiation lengths and have a resolution better than 3% for photons above 100 GeV [18]. Arm1 and Arm2 have different transverse size of the calorimeters and use different detectors for the measurement of the transverse position: Arm1 employs arrays of GSO scintillator bars, while Arm2 uses silicon microstrip detectors. The position resolution of the silicon microstrip detectors for electromagnetic showers is 40μm [19], while for GSO bars is 200 μm [18]. The transverse size of the Arm1 calorimeters is 20×20 mm^2 ("small tower") and 40×40 mm^2 ("large tower"), while for Arm2 it is 25×25 mm^2 ("small tower") and 32×32 mm^2 ("large tower"). The small tower of both Arm1 and Arm2 is placed on the beam line. A schematic view of both detectors can be seen in Figures 1 and 2

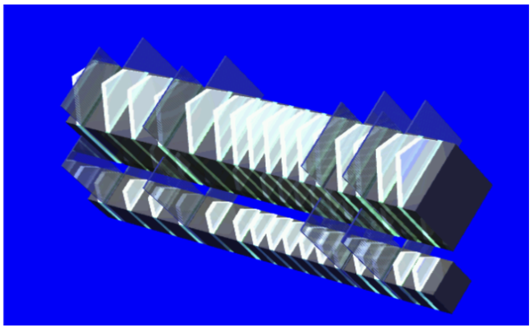

Figure 1: Schematic view of the Arm1 detector.

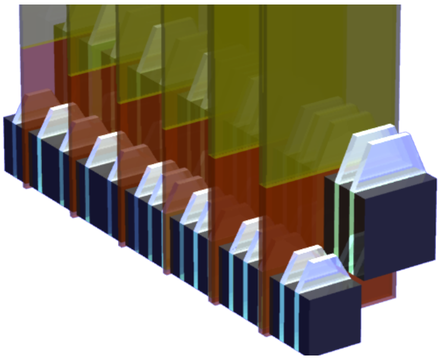

Figure 2: Schematic view of the Arm2 detector.

3. π^0 event reconstruction

The π^0 transverse momentum (p_T) and Feynman-X ($X_F \equiv 2p_Z/\sqrt{s}$) are reconstructed from the energy and impact position of the decay photons into the LHCf towers. Two typology of events can be recorded: "Type I" events where one photon hits each tower, and "Type II" events where both photons hit the same tower. In Type II events the energy deposited in the calorimeter is shared between the two photons using the information on the transverse profile of the showers provided by the position sensitive layers. Type I and Type II analyses are carried out independently and the comparison of the results will be shown in Section 4.

3.1 Event selection

A preselection is applied to the data to select the π^0 candidates:

- Energy threshold: events with an energy deposit corresponding to a photon with an energy > 200 GeV are selected. This requirement ensures a ∼100% trigger efficiency for both Arm1 and Arm2 detectors.
- Fiducial border: particles hitting the calorimeter within 2 mm from the border are rejected since the energy is not well reconstructed due to the high leakage of the shower outside the calorimeter.
- Particle identification (PID): in order to discriminate photon events from hadron events, the $L_{90\%}$ parameter is defined as the depth within 90% of the energy deposit is contained. all events with $L_{90\%}$ below a given threshold ($L^{thr}_{90\%}$) are selected as photon-like events. $L^{thr}_{90\%}$ is computed as an energy-dependent function to ensure a 90% π^0 selection efficiency according to Monte Carlo simulations. Different thresholds are computed for Type I and Type II events.

- Multi-hit rejection: events with at least a background particle in addition to the two photons are rejected: Type I events are rejected if there is more than one particle in a tower, while Type II events are rejected if there are three or more particles in the tower of interest.

3.2 Background subtraction

After the preselection, the invariant mass distribution ($M_{\gamma\gamma}$) of the two photons is built in each X_F bin to select π^0 events and to subtract the remaining background. The $M_{\gamma\gamma}$ distribution is fitted modelling the signal component as an asymmetric Gaussian and the background as a 3rd order polynomial. A signal window is defined as the $M_{\gamma\gamma}$ region within 3σ from the signal peak, while two background windows are defined between 4σ and 7σ from the peak. An example of the fit, including signal and background windows, is shown in Figure 3.

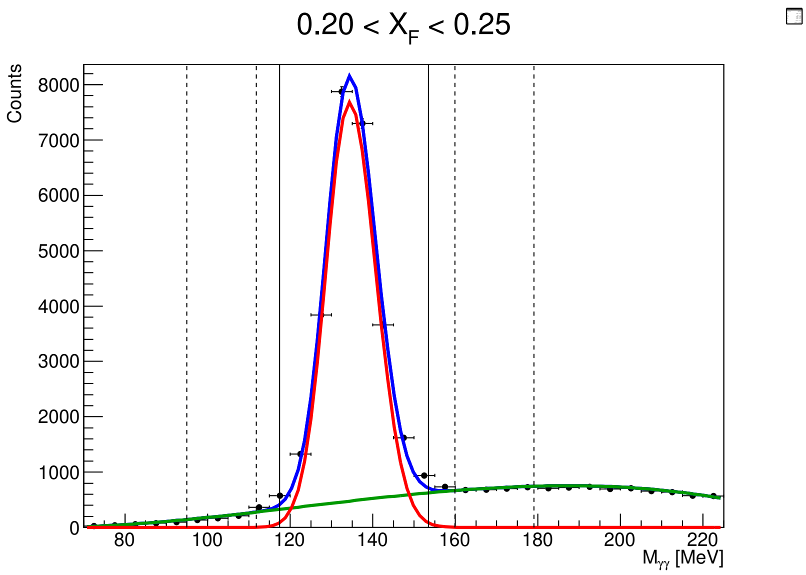

Figure 3: Invariant mass distribution for Arm2 Type-I events with $0.20 < X_F < 0.25$. The fit function is drawn as a blue line, while the signal and background components are plotted in red and green, respectively. The edges of the signal window are represented by the black vertical solid lines, while the background windows edges are drawn as black vertical dotted lines.

The signal p_T spectrum is obtained selecting the events in the signal window. The p_T distribution of the background is estimated selecting the events falling in background windows ("sideband method"). The absolute normalization of the background is obtained by scaling the background distribution by the ratio of the background function integral within the signal window and the background function integral in the background windows. The background distribution is finally subtracted from the signal spectrum.

3.3 Unfolding and corrections

In order to correct for the inefficiencies of the selection criteria and for the effects of the detector response, an iterative unfolding procedure based on the Bayes' theorem [20] is performed.

The response function for the unfolding was build for a simulated sample of π^0 with an uniform distribution in the p_T-X_F phase space. The simulation implements the π^0 decay near the IP1, the propagation of the photons from the decay position to the detector, and finally the interaction of the photons with the calorimeters. The COSMOS and EPICS [21, 22] Monte Carlo simulation codes were used for the interaction with the detector. Finally, the unfolded spectra are corrected for the geometrical acceptance of the towers. The geometrical acceptance map was generated with a dedicated toy Monte Carlo simulation. The geometrical acceptance of Arm2 is shown in Figures 4 and 5, where the complementary coverage of Type I and Type II events can be appreciated.

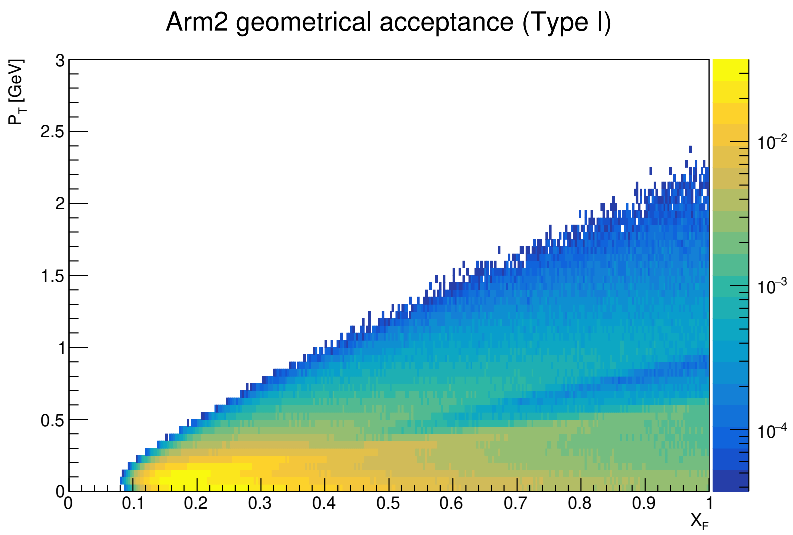

Figure 4: Arm2 geometrical acceptance for Type I π^0 events.

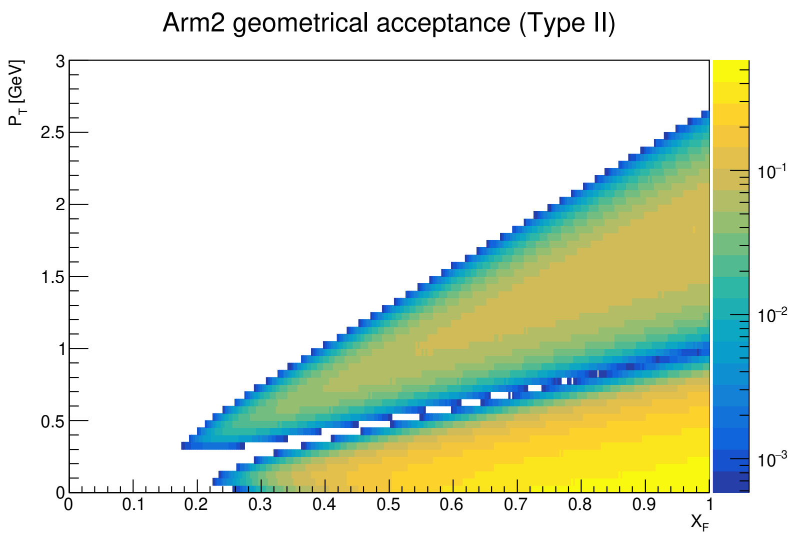

Figure 5: Arm2 geometrical acceptance for Type II π^0 events.

4. Results

The data set used in the analysis has been taken during the LHCf operation in proton-proton collisions at $\sqrt{s}$ = 13 TeV in LHC fill #3855. A dedicated low-luminosity beam setup was used. In the first ~3 hours of data taking a luminosity of ~0.4 $\times 10^{29}$ cm^{-2} s^{-1} was used, while in the next ~11 hours the luminosity was increased to ~1.4 $\times 10^{29}$ cm^{-2} s^{-1}. A dedicated trigger was used for Type I events (without the prescaling factor of the standard trigger) to increase their statistics. The integrated luminosity is ~2.1 nb^{-1} and ~0.8 nb^{-1} for Type I and Type II events, respectively.

The preliminary p_T spectra in several X_F bins are shown in Figure 6. Type I and Type II analyses provide results in good agreement in the regions where they overlap. Arm1 and Arm2 data also appear to be consistent with each other. The consistency of the data between different detectors and event types permits to fully take advantage of the different p_T and X_F coverage of Arm1 and Arm2, and of Type I and Type II events. Indeed, thanks to the larger dimension of its large tower, Arm1 is able to reach a larger p_T with respect to Arm2. Conversely, Arm2 close the gaps of Arm1 acceptance for X_F < 0.6 and extend the low-p_T coverage for X_F > 0.6 thanks to the larger dimension of its small tower. The inclusion of the data with the detectors shifted up by 5 mm with respect to the nominal position (aligned to the beam line) is expected to further reduce the remaining gaps in acceptance.

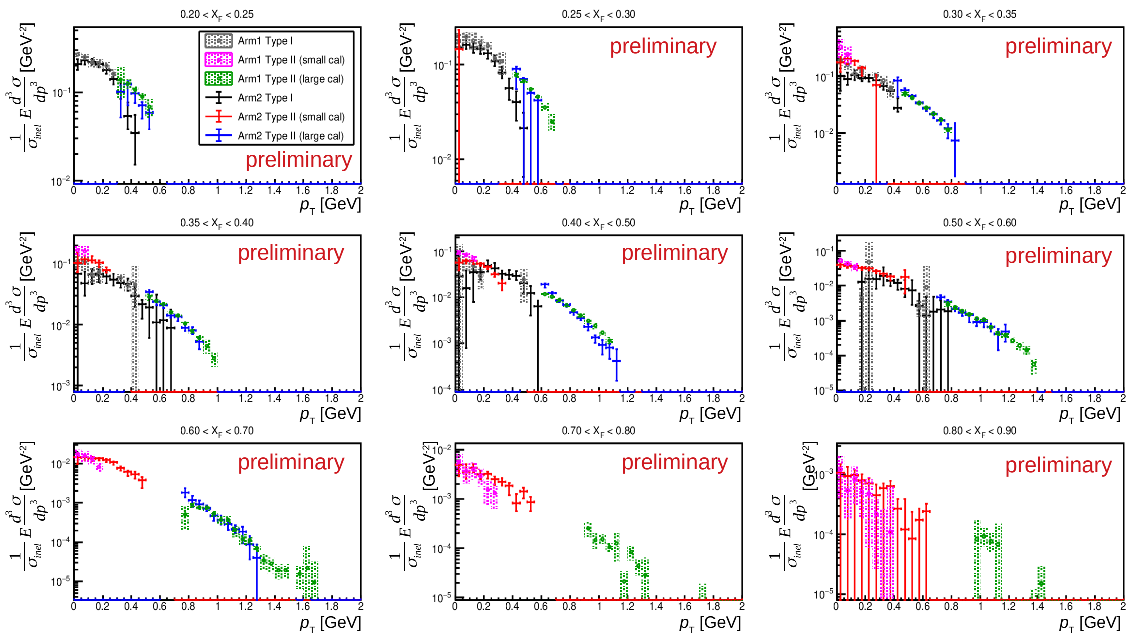

Figure 6: Transverse momentum spectra in different X_F bins measured with the Arm1 and Arm2 detectors of LHCf. Results from different detectors and π^0 event types are shown with different colors. Errors bars represent the total estimated uncertainty (statistical + systematic).

References

[1] *The pierre auger cosmic ray observatory*, Nuclear Instruments and Methods in Physics Research Section A: Accelerators, Spectrometers, Detectors and Associated Equipment **798** (2015) 172.

[2] M. Fukushima, *Telescope Array Project for Extremely High Energy Cosmic Rays*, Progress of Theoretical Physics Supplement **151** (2003) 206.

[3] Pierre Auger Collaboration collaboration, *Depth of maximum of air-shower profiles at the pierre auger observatory. i. measurements at energies above* $10^{17.8}$ eV, Phys. Rev. D **90** (2014) 122005.

[4] R. Abbasi, M. Abe, T. Abu-Zayyad, M. Allen, R. Anderson, R. Azuma et al., *Study of ultra-high energy cosmic ray composition using telescope array's middle drum detector and surface array in hybrid mode*, Astroparticle Physics **64** (2015) 49.

[5] V.N. Gribov, *A reggeon diagram technique*, *Sov. Phys. JETP* **26** (1968) 414.

[6] T. Regge, *Introduction to complex orbital momenta*, Il Nuovo Cimento **14** (1959) 951.

[7] L. Evans, *The Large Hadron Collider*, *New Journal of Physics* **9** (2007) 335.

[8] O. Adriani, L. Bonechi, M. Bongi, G. Castellini, R. D'Alessandro, D.A. Faus et al., *The LHCf detector at the CERN large hadron collider*, Journal of Instrumentation **3** (2008) S08006.

[9] O. Adriani et al., *Measurement of zero degree inclusive photon energy spectra for* $\sqrt{s}$ = 900 *GeV proton–proton collisions at LHC*, Physics Letters B **715** (2012) 298 .

[10] O. Adriani et al., *Measurement of zero degree single photon energy spectra for* $\sqrt{s}$ = 7 *TeV proton–proton collisions at LHC*, Physics Letters B **703** (2011) 128 .

[11] O. Adriani, E. Berti, L. Bonechi, M. Bongi, R. D'Alessandro, M. Haguenauer et al., *Measurement of forward photon production cross-section in proton–proton collisions at* $\sqrt{s}$ *= 13 TeV with the LHCf detector*, Physics Letters B **780** (2018) 233.

[12] O. Adriani et al., *Measurement of very forward neutron energy spectra for 7 TeV proton–proton collisions at the Large Hadron Collider*, Physics Letters B **750** (2015) 360 .

[13] O. Adriani, E. Berti, L. Bonechi, M. Bongi, R. D'Alessandro, S. Detti et al., *Measurement of inclusive forward neutron production cross section in proton-proton collisions at* $\sqrt{s}$ = 13 *TeV with the LHCf Arm2 detector*, Journal of High Energy Physics **2018** (2018) 73.

[14] O. Adriani, E. Berti, L. Bonechi, M. Bongi, R. D'Alessandro, S. Detti et al., *Measurement of energy flow, cross section and average inelasticity of forward neutrons produced in* $\sqrt{s}$ = 13 *TeV proton-proton collisions with the LHCf Arm2 detector*, Journal of High Energy Physics **2020** (2020) 16.

[15] The LHCf Collaboration collaboration, *Measurement of forward neutral pion transverse momentum spectra for $\sqrt{s}$ = 7 TeV proton-proton collisions at the LHC*, Phys. Rev. D **86** (2012) 092001.

[16] LHCf Collaboration collaboration, *Transverse-momentum distribution and nuclear modification factor for neutral pions in the forward-rapidity region in proton-lead collisions at $\sqrt{s_{NN}}$ = 5.02 TeV*, Phys. Rev. C **89** (2014) 065209.

[17] LHCf collaboration, *Measurements of longitudinal and transverse momentum distributions for neutral pions in the forward-rapidity region with the LHCf detector*, Phys. Rev. **D94** (2016) 032007 [1507.08764].

[18] Y. Makino, A. Tiberio, O. Adriani, E. Berti, L. Bonechi, M. Bongi et al., *Performance study for the photon measurements of the upgraded LHCf calorimeters with gd2sio5(GSO) scintillators*, Journal of Instrumentation **12** (2017) P03023.

[19] O. Adriani, L. Bonechi, M. Bongi, G. Castellini, R. Ciaranfi, R. D'Alessandro et al., *The construction and testing of the silicon position sensitive modules for the LHCf experiment at CERN*, *Journal of Instrumentation* **5** (2010) P01012.

[20] G. D'Agostini, *A multidimensional unfolding method based on Bayes' theorem*, *Nuclear Instruments and Methods in Physics Research Section A: Accelerators, Spectrometers, Detectors and Associated Equipment* **362** (1995) 487 .

[21] K. Kasahara, *Introduction to Cosmos and some relevance to ultra high energy cosmic ray air showers*, *Proceedings of 24th International Cosmic Ray Conference, Rome* **1** (1995) 399.

[22] K. Kasahara, *Cosmos and Epics web page*, *http://cosmos.n.kanagawa-u.ac.jp* .

Full Authors List: LHCf Collaboration

O. Adriani[a,b], E. Berti[a,b], L. Bonechi[a], M. Bongi[a,b], R. D'Alessandro[a,b], G. Castellini[c], M. Haguenauer[d], Y. Itow[ef], K. Kasahara[g], M. Kondo[e], Y. Matsubara[e], H. Menjo[e], Y. Muraki[e], K. Ohashi[e], P. Papini[a], S. Ricciarini[a,c], T. Sako[h], N. Sakurai[i], K. Sato[e], Y. Shimizu[j], T. Tamura[k], A. Tiberio[a], S. Torii[k], A. Tricomi[l,m,n], W. C. Turner[o], M. Ueno[e], K. Yoshida[g]

[a] INFN Section of Florence - Florence, Italy
[b] University of Florence - Florence, Italy
[c] IFAC-CNR - Florence, Italy
[d] Ecole-Polytechnique - Palaiseau, France
[e] Institute for Space-Earth Environmental Research - Furo-cho, Chikusa-ku, Nagoya, Japan
[f] Kobayashi-Maskawa Institute for the Origin of Particles and the Universe, Nagoya University - Nagoya, Japan
[g] Faculty of System Engineering, Shibaura Institute of Technology, Japan
[h] Institute for Cosmic Ray Research, University of Tokyo, Chiba, Japan
[i] Tokushima University, Tokushima, Japan
[j] Kanagawa University - Kanagawa, Japan
[k] RISE, Waseda University - Shinjuku, Tokyo, Japan
[l] INFN Section of Catania - Catania, Italy
[m] University of Catania - Catania, Italy
[n] CSFNSM, Catania, Italy
[o] LBNL - Berkeley, California, USA